Surface Soil Moisture Retrieval and Mapping Using High-Frequency Microwave Satellite Observations in the Southern Great Plains

THOMAS J. JACKSON AND ANN Y. HSU

USDA-ARS Hydrology and Remote Sensing Laboratory, Beltsville, Maryland

PEGGY E. O'NEILL

Hydrological Sciences Branch, Laboratory for Hydrospheric Processes, NASA Goddard Space Flight Center, Greenbelt, Maryland

(Manuscript received 16 November 2001, in final form 10 July 2002)

ABSTRACT

Studies have shown the advantages of low-frequency (<5 GHz) microwave sensors for soil moisture estimation. Although higher frequencies have limited soil moisture retrieval capabilities, there is a vast quantity of systematic global high-frequency microwave data that have been collected for 15 yr by the Special Sensor Microwave Imager (SSM/I). SSM/I soil moisture studies have mostly utilized antecedent precipitation indices as validation, while only a few have employed limited ground observations, which were typically not optimal for this particular type of satellite data. In the Southern Great Plains (SGP) hydrology experiments conducted in 1997 and 1999, ground observations of soil moisture were made over an extended region for developing and validating large-scale mapping techniques. Previous studies have indicated the limitations of both the higher-frequency data and models for soil moisture retrieval. Given these limitations, an alternative retrieval technique that utilizes multipolarization observations was implemented and tested for the SGP region. A technique for extracting algorithm parameters from the observations was developed and tested. The algorithm was then used to produce soil moisture maps of the region for the two study periods.

1. Introduction

The potential of passive microwave remote sensing for measuring surface soil moisture has been demonstrated over a range of microwave frequencies (Choudhury and Golus 1988; Paloscia et al. 1993; Lakshmi et al. 1997; Drusch et al. 2001) and a variety of platforms (Wang 1985; Jackson et al. 1999; Jackson and Hsu 2001). These studies clearly show the advantages of low-frequency (<5 GHz) microwave sensors for this application. Although low-frequency sensors are recognized as the best direction for future soil moisture measurement systems, there is still a good reason in the meantime to consider the use of higher frequencies: the vast quantity of global systematic high-frequency microwave data that have been collected for the past 15 yr by the Special Sensor Microwave Imager (SSM/I).

Despite the fact that high-frequency microwave sensors will have limited retrieval capabilities, there are some conditions under which these observations can provide useful soil moisture information. Most studies using SSM/I and other passive microwave satellite systems to estimate soil moisture have utilized antecedent precipitation indices (APIs) as validation (Choudhury and Golus 1988; Ahmed 1995; Teng et al. 1993; Owe et al. 1992). Morland et al. (2001) compared APIs to soil moisture in estimating SSM/I emissivity. In that study they found APIs to be less correlated to emissivity and concluded that rapid drying of the soil layer, which determines the microwave emission was not adequately reflected in APIs.

A few investigations have employed limited observations from ground networks that were not optimally designed for this particular type of satellite data. The ground networks were either sparse, such as in Koike et al. (2000) (one measurement station per one SSM/I footprint) and in Vinnikov et al. (1999) (17 soil moisture stations for the entire state of Illinois), or the soil moisture layer observed was much deeper than that which determines the microwave response, such as in Owe et al. (1992) (20 cm) and in Vinnikov et al. (1999) (10 cm).

As part of the Southern Great Plains (SGP) hydrology experiments conducted in 1997 (SGP97) and 1999 (SGP99), ground observations of soil moisture were made over an extended region in order to contribute to the validation and demonstration of large-scale mapping of soil moisture using SSM/I data. In a previous investigation the use of a single-channel soil moisture retrieval algorithm was evaluated with limited datasets collected over the region in 1992 and 1994 (Jackson 1997). An investigation by Drusch et al. (2001) used the SGP97 SSM/I data and a more sophisticated radi-

Corresponding author address: Dr. Thomas Jackson, USDA-ARS Hydrology and Remote Sensing Lab, 104 Building 007, BARC-West, Beltsville, MD 20705.
E-mail: tjackson@hydrolab.arsusda.gov

TABLE 1. SSM/I satellite platforms.

Satellite	Dates of operation	Ascending equatorial crossing time (UTC)
F8	Jun 1987–Apr 1994	0612
F10	Dec 1990–Nov 1997	2215
F11	Nov 1991–May 2000	1925
F13	Mar 1995–present	1754
F14	Apr 1997–present	2046
F15	Dec 1999–present	2120
F16	2003 launch	TBD

ative transfer approach that fully considered atmospheric effects to study soil moisture and brightness temperature relationships.

These previous studies have indicated the limitations of both the high-frequency data and the models used for soil moisture retrieval. In the current investigation an alternative retrieval technique utilizing multipolarization observations and based upon the work of Njoku and Li (1999) was implemented and tested for the SGP region. Available information on parameters needed by the soil moisture retrieval algorithm at high frequencies is lacking. As part of the current investigation, a technique for extracting algorithm parameters from the observations was developed and tested. The algorithm was then used to produce soil moisture maps of the region for the two study periods.

2. The SSM/I instrument

The SSM/I is a conical scanning total power microwave radiometer system operating at a look angle of 53° at four frequencies: 19.4, 22.2, 37, and 85.5 GHz. The 22.2-GHz channel operates in V polarization and the other three channels in both V and H polarization. Spatial resolution [effective field of view (EFOV) 3-dB beamwidth] ranges from 69 km by 43 km at 19.4 GHz to 15 km by 13 km at 85.5 GHz. The orbital period is about 102 min, which results in 14.1 orbits per day. For a given satellite, coverage is possible twice a day approximately 12 h apart on the ascending and descending passes. Additional information can be found in Hollinger et al. (1990).

SSM/I instruments have been a component of the Defense Meteorological Satellite Program since 1987. Table 1 summarizes some aspects of the data records available from this series of satellites.

3. Soil moisture retrieval algorithm

a. Brightness temperature modeling

Recent efforts to develop soil moisture retrieval algorithms for the Advanced Microwave Scanning Radiometer (AMSR) instruments on the National Aeronautics and Space Administration (NASA) *Aqua* and National Space Development Agency of Japan (NASDA) *Advanced Earth Observing Satellite-II* (*ADEOS-II*) satellites (Njoku et al. 2000; Koike et al. 2000) have resulted in the formalization of several alternative approaches for microwave soil moisture estimation from space. For the most part, all of these methods are based upon the same basic radiative transfer equation for a specific frequency and polarization. The formulation used here follows that of Drusch et al. (2001) for a soil target with a vegetation canopy at a specific frequency:

$$\begin{aligned} T_B^p = {} & T_{\text{au}} + \exp(-\tau_{\text{atm}})[T_{\text{ad}} + T_{\text{sky}} \exp(-\tau_{\text{atm}})](1 - \varepsilon^p) \\ & \times \exp(-2\tau_{\text{veg}}^p) + \exp(-\tau_{\text{atm}}) \\ & \times \{\varepsilon^p T_{\text{soil}} \exp(-\tau_{\text{veg}}^p) \\ & + T_{\text{veg}}(1 - \omega_{\text{veg}}^p)[1 - \exp(-\tau_{\text{veg}}^p)] \\ & \times [1 + (1 - \varepsilon^p) \exp(-\tau_{\text{veg}}^p)]\}, \end{aligned} \tag{1}$$

where T_B is brightness temperature (K), T_{au} is upward atmospheric brightness temperature contribution (K), T_{ad} is downward atmospheric brightness temperature contribution (K), T_{sky} is sky brightness temperature (K), T_{soil} is soil temperature (K), T_{veg} is vegetation temperature (K), τ_{atm} is optical depth of the atmosphere (Np), τ_{veg} is optical depth of the vegetation (Np), ω_{veg} is single scattering albedo of the vegetation, ε is emissivity of the soil surface, and p is polarization of the measurement, horizontal or vertical.

The soil surface emissivity includes roughness effects that must be corrected for in order to estimate the soil emissivity. Following Choudhury et al. (1979),

$$\begin{aligned} \varepsilon^p = {} & 1 - [Q^p(1 - \varepsilon_0^H) + (1 - Q^p)(1 - \varepsilon_0^V)] \\ & \times \exp(-4k^2\sigma^2 \cos^2\theta), \end{aligned} \tag{2}$$

where Q is a polarization coupling factor that is polarization dependent, ε_0 is emissivity of the soil, k is wavenumber, σ is standard deviation of the surface height (cm), and θ is incident angle (°). The variables in the exponential of Eq. (2) are often represented by a single roughness parameter h.

The soil emissivity is 1 minus the reflectivity, which is computed using the Fresnel reflection equations as follows:

$$\varepsilon_0^H = 1 - \left| \frac{\cos\theta - \sqrt{k - \sin^2\theta}}{\cos\theta + \sqrt{k - \sin^2\theta}} \right|^2 \tag{3}$$

$$\varepsilon_0^V = 1 - \left| \frac{k\cos\theta - \sqrt{k - \sin^2\theta}}{k\cos\theta + \sqrt{k - \sin^2\theta}} \right|^2, \tag{4}$$

where k is the complex dielectric constant of the soil, which is related to the volumetric soil moisture using a dielectric mixing model. There are several formulations that are commonly used (Wang and Schmugge 1980; Hallikainen et al. 1985; Dobson et al. 1985), each of which requires the specification of a particular set of input parameters. The Wang and Schmugge (1980) formulation was developed based on measurements at 1.4 and 5 GHz. The formulation by Hallikainen et al. (1985)

and Dobson et al. (1985) used the same measurements taken over the 1–18-GHz region. Hallikainen et al. (1985) is a semiempirical mixing model that describes the data accurately and requires only volumetric moisture and soil texture as inputs. Dobson et al. (1985) is a theoretical four-component mixing model that explicitly accounts for the effect of bound water.

b. Atmospheric correction

Equation (1) contains three atmospheric parameters: T_{au}, T_{ad}, and τ_{atm}. The first two, T_{au} and T_{ad}, are the integrals of the atmospheric temperature profile, and the third one, τ_{atm}, is the cumulative optical depth. Since neither the temperature nor the humidity profiles of the atmosphere are symmetrically stratified, differences can occur between integrating from the top of the atmosphere down and from the earth's surface up. Drusch et al. (2001) analyzed data from 1997 in this region and found that the values of T_{au} and T_{ad} could be assumed to be equal with very little impact on the computations of brightness temperature, especially for 19 and 37 GHz.

The optical depth, τ_{atm}, is the integral of the atmospheric absorption coefficient profile. Under cloud-free conditions at lower frequencies the atmospheric absorption coefficient (α, in decibels per kilometer) is primarily due to atmospheric water vapor and oxygen. Although there are several models available that describe the absorption as a function of frequency and the properties of the profile, Drusch et al. (2001) found that the differences introduced in the computations from using these attenuation models were negligible and chose to use Liebe et al. (1993). These absorption models utilize the temperature, atmospheric pressure, and water vapor density of the atmospheric profile layers.

c. Vegetation effects

Vegetation effects on the microwave radiometric sensitivity to soil moisture have been studied by various researchers (e.g., Kirdiashev et al. 1979; Jackson and Schmugge 1991; Ulaby et al. 1983; Calvet et al. 1995). Many of these studies have been based on data collected by truck-mounted radiometers over a single specific type of vegetation (Jackson and Schmugge 1991; Pampaloni and Paloscia 1986; Paloscia and Pampaloni 1992; Calvet et al. 1995). However, more than one type of vegetation will often be found in a large satellite footprint. It is also difficult to apply theoretical vegetation models (Calvet et al. 1995) that require many parameters to account for the vegetation contribution to the microwave emission from the earth's surface.

Jackson and Schmugge (1991) described a semiempirical approach to estimating vegetation effects that could be applied over a range of frequencies. In that investigation the optical depth of the vegetation (τ_{veg}) was related to a parameter b and the vegetation water content (W_{veg}). The parameter b was found to vary in a systematic manner with frequency. However, they found that the variability in this parameter, which was associated with canopy structure, also increased with frequency. This suggests that a priori estimates of vegetation parameters using this approach are less reliable at the SSM/I frequencies than at L band.

d. Algorithm alternatives

Equations (1)–(4) involve many variables and parameters. In Njoku and Li (1999) these were categorized as either media or media and sensor variables (dependent upon both frequency and polarization of the sensor). The only media variables are those describing the physical temperatures of the scene constituents and the atmospheric profile. Solving Eqs. (1)–(4), either forward calculations of T_B or inversions for soil moisture, requires assumptions and/or ancillary data to reduce the dimensionality of the problem. Adding additional channels of observations (polarization or frequency) will only help in the solution if they do not increase the number of unknowns in the equations.

Most research and applications involving passive microwave remote sensing of soil moisture have emphasized low frequencies (L band). In this range, it is possible to develop soil moisture retrievals based on single-channel H-polarization observations (Jackson 1993). This approach relies on providing ancillary data on temperature, vegetation, land cover, and soils. Atmospheric corrections are assumed to be negligible at these low frequencies.

In Jackson (1997) the single-channel/ancillary data approach was extended to the higher frequencies of the SSM/I instrument. A simple approximation of the required atmospheric corrections was applied to the dataset before attempting to relate soil moisture observations and emissivity. For the limited validation dataset available, the approach performed relatively well, with a standard error of estimate of 5.3%. It is likely that the success of the approach was related to the limited conditions and light vegetation conditions evaluated.

As noted previously, the optical depth computation approach used in Jackson and Schmugge (1991) has a high degree of uncertainty at higher frequencies. In addition, other investigators have found that the vegetation single-scattering albedo must be considered at high frequencies (Njoku and Li 1999; Owe et al. 1992).

It is the weakness of the vegetation correction that initiated reconsidering the application of the single-channel/ancillary data algorithm when using high-frequency microwave data for soil moisture estimation. As a result we examined a variation of the approach proposed in Njoku and Li (1999). In this approach, a series of equations for predicting the brightness temperature of several channels is solved iteratively. Several channels (polarizations and/or frequencies) can be used, subject to the constraint that the number of unknowns is less than or equal to the number of equations. Our im-

plementation of this approach is based upon the following assumptions.

1) Atmospheric effects
   - Data are available to perform atmospheric corrections [T_{au}, T_{ad}, and τ_{atm} in Eq. (1)].
2) Target temperature
   - Effective soil temperature at the time of observation can be accurately estimated using ancillary data sources; this value represents both the soil and vegetation temperatures [T_{soil} and T_{veg} in Eq. (1)].
3) Vegetation effects
   - Vegetation optical depth cannot be estimated a priori at high frequencies using ancillary data.
   - Vegetation optical depth is frequency dependent.
   - Vegetation optical depth at 19 GHz is smaller and less significant than at 37 GHz; therefore, if choosing a single SSM/I frequency, 19 GHz is preferred.
   - Vegetation optical depth at high frequencies is not polarization dependent.
   - Vegetation water content can be determined based on field measurements of major vegetation types and optical satellite images.
   - The single scattering albedo is polarization dependent and can be estimated a priori from ancillary data.

With these specifications, the unknowns in Eq. (1) reduce to the emissivity [and consequently to the dielectric constant of soil by Eqs. (3) and (4)] and vegetation optical depth, which is specified as being independent of polarization. At lower frequencies and higher spatial resolution, the vegetation optical depth is a function of the vegetation water content for a particular crop structure (Kirdiashev et al. 1979):

$$\tau_{veg} = bW_{veg}. \quad (5)$$

At SSM/I frequencies and spatial resolutions the b parameter needs to be determined analytically. It is also specified that all parameters in Eq. (2) can be estimated a priori and that soil property information is available to link the dielectric constant to the soil moisture via the dielectric mixing model.

With dual-polarization 19-GHz data from the SSM/I there will be two observed variables and radiative transfer equations that depend on two unknowns. The solution of these is through optimization with some constraints based upon published results. The impact of some of the assumptions mentioned will be examined in later sections.

4. Southern Great Plains 1997 and 1999 hydrology experiments

SGP97 and SGP99 were interdisciplinary science experiments that included the objective of validating the hypothesis that retrieval algorithms for surface soil moisture developed at higher spatial resolution using truck- and aircraft-based sensors can be extended to the coarser resolutions expected from satellite platforms (Jackson et al. 1999; Jackson and Hsu 2001). Experiments took place from 18 June to 17 July 1997 and 6 July to 20 July 1999 in Oklahoma. The area covered ranged from the Little Washita River watershed in the south to the Department of Energy (DOE) Central Facility for the Atmospheric Radiation Measurement (ARM) Program near the Kansas border in the north. Extensive ground measurements of soil moisture were collected within the Little Washita watershed (LW), the Central Facility area (CF), and the U.S. Department of Agriculture (USDA) Grazinglands Research Laboratory at El Reno (ER) west of Oklahoma City (Fig. 1).

The Little Washita watershed covers an area of 603 km^2. Soils include a wide range of textures, with large regions of both coarse and fine textures. Land use is dominated by rangeland and pasture (63%), with significant areas of winter wheat and other crops concentrated in the floodplain and western portions of the watershed area. The El Reno area consists of 24.3 km^2 of government-operated grasslands. Generally, this area is a mixture of grasslands and winter wheat. However, most of the grasslands in the El Reno area are ungrazed and have significantly greater biomass than the other two intensive measurement areas. The area surrounding the Central Facility site is dominated by winter wheat, which was ready for harvest or harvested (wheat stubble) during the experiments.

Soil moisture sampling of the surface soil layer was carried out in fields approximately a quarter section (0.8 km by 0.8 km) in size distributed over each of the study areas. The sampling performed in these fields involved two transects separated by 400 m with a sample every 100 m, resulting in 14 samples per field. In addition, other smaller sites were sampled. In 1997 there were 20 sites sampled in the LW, 15 in the ER, and 9 in the CF. During 1999 there were 6 sites in CF, 6 in ER, and 20 in LW. The results for each field in a particular area were averaged together to compute a single average soil moisture value for that area on a given day.

In addition to soil moisture, measurements of vegetation characteristics and roughness parameters were made. In 1997, the average value of the vegetation water content over the sampled fields was 0.37 kg m^{-2} for the CF, about 0.59 kg m^{-2} for the ER, and about 0.43 kg m^{-2} for LW.

Data from two instrument networks were used in the current study: meteorological data from the Oklahoma Mesonet and radiosonde observations from the DOE ARM. The Oklahoma Mesonet consists of 114 automated stations covering the entire state. At each station, the local environment is measured by a set of instruments located on or near a 10-m-tall tower. Measurements included air and soil temperatures at 5- and 15-min intervals, respectively.

Within the ARM region, routine radiosonde launches take place at the Central Facility and four boundary facilities (three of these are shown in Fig. 1; the other

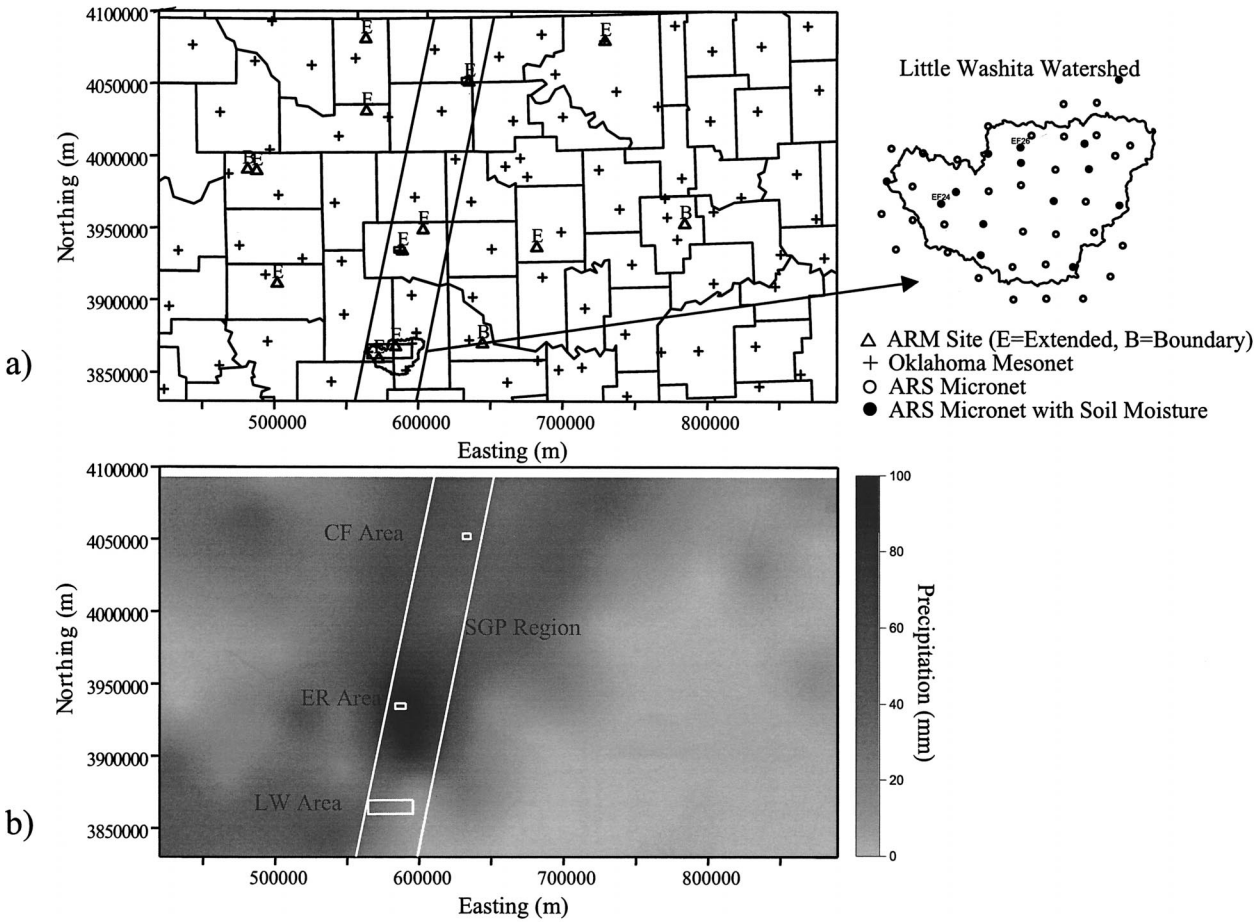

FIG. 1. Maps of SGP study area (a) related instrument networks and (b) cumulative rainfall for 9–10 Jul 1999.

is in Kansas). The routine schedule at the CF was 0600, 1200, 1500, 1800, and 2100 UTC, and at the boundary facilities only at 1800 UTC (i.e., at the local noon). During SGP97 and SGP99, which were intensive observation periods, CF and all boundary facilities had launches beginning at 0230 UTC and then every 3 h until 2330 UTC.

5. Data processing and algorithm implementation

A total of 80 SSM/I datasets were available from SGP97 and 27 from SGP99, which were a subset of all possible passes that satisfied spatial coverage and experiment requirements. These data were transferred from the National Oceanic and Atmospheric Administration (NOAA) National Environmental Satellite, Data, and Information Service (NESDIS) in the form of antenna temperatures. Latitude–longitude coordinates for each footprint are included with these records. Datasets were processed to eliminate scans without coverage in the SGP region and to convert the antenna temperatures to brightness temperatures. The boundary of this common study region ranges from 34° to 38.5°N and from 98.5° to 96.6°W, or from 543 600 E to 708 400 E and from 3 764 200 N to 4 261 000 N in UTM 14S with Clarke 1886 datum.

a. Atmospheric parameters

Ideally, radiosonde observations at the exact time and place of each satellite observation should be used as input to the computation of the atmospheric parameters. For this study, we used the radiosonde observations provided by the ARM Program. Atmospheric profiles derived from balloon soundings at the CF during the study periods were obtained from the ARM archive. If the SSM/I overpass was within 30 min of a radiosonde observation, that dataset was used for computing atmospheric correction parameters. Otherwise, the observations right before and after the SSM/I overpass were linearly interpolated to the time of the SSM/I overpass. The three variables required to compute the absorption coefficients (air temperature, atmospheric pressure, and relative humidity) were extracted and used to compute atmospheric transmissivity following Drusch et al. (2001). The value of T_{au} was integrated based on the atmospheric temperature profiles and assumed equal to T_{ad}.

b. Effective soil temperature

Effective soil temperature was computed following Choudhury et al. (1982) using data collected by the Oklahoma Mesonet. Air temperature measured at 1.5-m height was used to estimate surface temperature, and soil temperature measured at 10-cm depth under the sod was used for the deep soil temperature. The values collected closest in time to each SSM/I overpass were selected and used to compute T_{soil} at each station. For each overpass these data were used in a grid interpolation program to produce an 800-m-resolution data product. The center and extent of each SSM/I footprint were used with these 800-m products to extract the average T_{soil}.

The use of air temperature to represent the effective temperature of the emitting layer is accurate when the temperature profile of the land and near-surface air is in equilibrium. This occurs in the early morning hours. Differences and potential errors are larger in late afternoon and depend upon conditions on a given day. We chose to use all the available SSM/I data and accept this potential error. At higher frequencies, such as 19 GHz, the 10-cm soil temperature is less important in the retrieval than it is at lower frequencies.

c. Land cover and vegetation

Land cover classification maps developed as part of the SGP experiments using Landsat Thematic Mapper (TM) data were used to characterize the constituents of vegetation for each SSM/I footprint. The center of each SSM/I footprint was located on land cover maps, and the extent of the footprint was used to extract the percentage of each land cover category in the footprint. Ground measurements of vegetation water content for the major vegetation types found within the study area were then used with the land cover information to compute the vegetation water content in each SSM/I footprint (percent of land cover class in footprint times measured water content for that type of vegetation). Since each TM pixel was assigned to a land cover class based on the predominant type, the computed vegetation water content could be under- or overestimated. To verify this, the average Normalized Difference Vegetation Index (NDVI) value based on data from Advanced Very High Resolution Radiometer (AVHRR) for the footprint was derived with the same integration procedure used to estimate the land cover categories of the footprint. If the computed vegetation water content in a footprint was low but the NDVI value for the footprint was high, the vegetation water content was adjusted proportional to the NDVI value.

d. Roughness parameters

Data for estimating surface roughness parameters are sparse. Here we used the results presented in Njoku and Li (1999) for Africa at 18 GHz to determine the values of Q and h used in Eq. (2). Extrapolation of these values to the entire SGP region may not be valid since land cover conditions are different. However, they should apply to the grassland areas in this study.

e. Soil characteristics and dielectric mixing model

The dielectric mixing model developed by Hallikainen et al. (1985) was used to convert volumetric soil moisture into soil dielectric constant for both forward and inverse modeling. This mixing model is valid for higher frequencies of the microwave range, and requires percent of sand and clay as input, in addition to volumetric soil moisture. The soil texture classification of the surface soil on a 1-km grid for the conterminous United States (http://www.essc.psu.edu/soil_info/) was used here. For each SSM/I footprint the soil texture properties were retrieved and averaged.

f. Algorithm implementation

A computer program was developed for the forward radiative transfer model that iteratively computes T_B for soil moisture values ranging from 5% to 45%, in 1% increments, and for the vegetation b factor from 0.6 to 1.2, in 0.025 steps. The single-scattering albedo was set as 0.0 for H polarization and was varied between 0.0 and 0.05 for V polarization following the work by Jackson (1997). At each iteration step, the computed T_B values for 19H and 19V were compared to the satellite observations. If the mean of the differences between the computed and observed T_B at 19H and 19V was less than 1.5 K, the input soil moisture, the computed T_B values, and the reflectivity of the two-layer soil/vegetation surface were saved in arrays. The soil moisture value in the array that provides computed emissivity closest to the measured SSM/I is then selected as the value for that footprint.

Results showed that the algorithm overestimated soil moisture when more than 40% of the surface in the footprint was covered by grass. The structure of grass plants is quite different from agricultural crops. To account for this difference the single-scattering albedo was set lower for grass. In addition, if over one-third of the area of a footprint was occupied by trees, water bodies, and/or was urban, the algorithm cannot provide a reasonable estimate of soil moisture for the footprint. These footprints were discarded from analysis.

6. SSM/I analyses and results

a. Emissivity and volumetric soil moisture

As the first step in analyzing the retrieval algorithm, we examined the relationships between emissivity and soil moisture. An emissivity estimate, which included atmospheric corrections, was computed for each footprint by dividing SSM/I T_B by the average effective

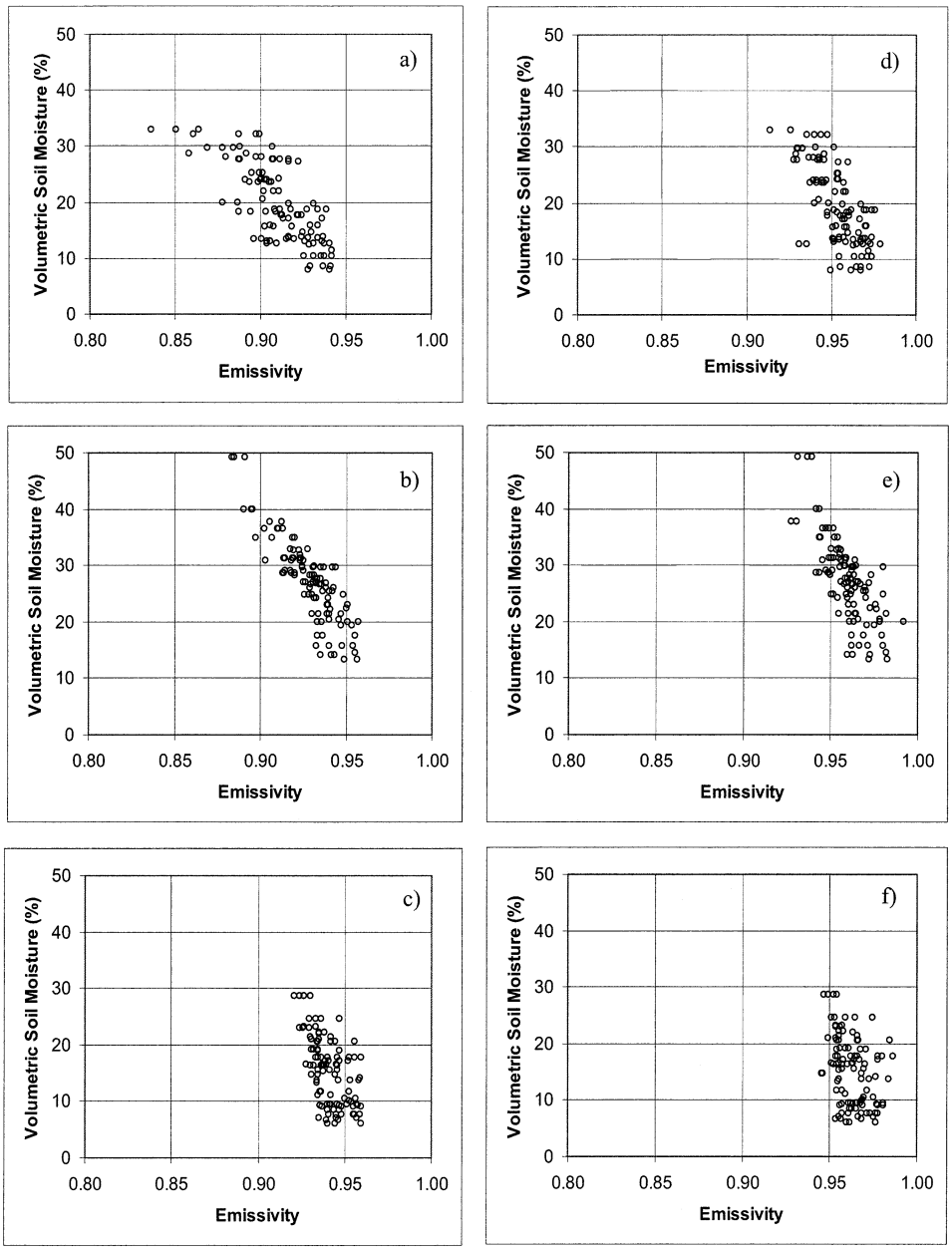

FIG. 2. Observed soil moisture and 19-GHz emissivity for the SGP study sites (a) CF H, (b) ER H, (c) LW H, (d) CF V, (e) ER V, and (f) LW V.

temperature in each footprint. Only the 19-GHz data are discussed here because they typically contain the most soil moisture information (Jackson 1997). These data were input to a mapping and interpolation routine that generated data on a uniform grid. Emissivity values for each of the three study areas (CF, ER, and LW) were then extracted by averaging all grid points within their respective boundaries.

Figure 2 shows the plots of the observed soil moisture and 19-GHz H and V emissivity values for all observations in SGP97 and SGP99. Each point in the plot represents an average value for the specific sampling area (i.e., CF, ER, or LW) on a given day. The soil moisture value is the average of all the sampling fields in that area. Average emissivity was computed from the gridded 800-m pixels that fell within the geographic boundary of each area. Although there is scatter in the data, the expected general linear trends are evident (Jackson 1997). Scatter appears to be larger for the CF site, which also has the largest dynamic range in emissivity. One explanation for this is the size of the area that was ground sampled (a few kilometers) versus the inherent resolution of the sensor and local variations in soil moisture. This was a small site in a region with

TABLE 2. Parameters for 19-GHz emissivity and soil moisture.

		Linear regression error	Algorithm parameter optimization					
			Parameters		Error descriptors		Algorithm error discriptors	
Polarization	Area	Standard error of estimate (%)	Composite vegetation and roughness (α)	Single-scattering albedo (ω)	Bias (%)	Standard error of estimate (%)	Bias (%)	Standard error of estimate (%)
H	CF	4.63	0.2365	—	0.45	7.11	0.28	5.14
	ER	3.57	0.1603	—	0.44	8.06	5.01	7.54
	LW	4.90	0.1699	—	0.27	5.08	1.48	6.10
V	CF	5.01	0.2365	0.05	−0.26	6.36	—	—
	ER	4.72	0.1603	0.04	−0.96	8.06	—	—
	LW	5.60	0.1699	0.05	1.45	7.70	—	—

high variability. The change in the general slopes of the relationships between emissivity and soil moisture supports theory and reflects the physical characteristics of the sites. The CF site with the least amount of vegetation has the largest sensitivity of soil moisture to emissivity.

The sensitivity of 19-GHz V emissivity data to soil moisture is less than that of 19-GHz H data in all three sampling areas. Correlation between the observed emissivity and soil moisture appears rather poor for LW H polarization. Among the three sampling areas, LW was the driest one, with maximum average volumetric soil moisture in the study period less then 30%. The effect of soil moisture on microwave emission is reflected through the dielectric constant of soils. Data collected at 18 GHz (Hallikainen et al. 1985) showed that the real part of the dielectric constant for five soils ranging from sandy loam to silty clay increased from 2.5 to about 11.5 when the volumetric soil moisture increased from very dry to 30%. In the range of soil moisture between 30% and 40%, the real part of the dielectric constant increased from 11.5 to 15. This faster increase in the dielectric constant at higher soil moisture may explain part of the poor correlation for LW.

Although it is not a robust approach, it can be informative to perform a linear regression on the emissivity and soil moisture data, which typically exhibit a linear trend. Results are summarized in Table 2 for the three sites. Standard error of estimate (SEE) values are on the order of those previously reported (Jackson 1997) and should be considered as a baseline for evaluating retrieval algorithm performance. Other data in Table 2 will be discussed in the following sections.

b. Optimizing algorithm parameters using observations

Using the assumptions specified earlier, it is possible to determine values of the vegetation parameters (τ_{veg} and ω_{veg}) from the SSM/I observations and soil moisture measurements. This is accomplished by using the emissivity estimates with a simplified form of Eqs. (3) and (4) and a dielectric mixing model.

Ignoring atmospheric effects for the moment, when $\omega_{veg} = 0$ the following relationship is found from Eq. (1):

$$(1 - \varepsilon_{obs}) = (1 - \varepsilon_{soil})^*\alpha. \quad (6)$$

Values of one minus the emissivity are equivalent to the reflectivity. Following the development presented in Schmugge et al. (1992), the value of the parameter α in this equation is defined as

$$\alpha = \exp(-h - 2\tau_{veg}), \quad (7)$$

where h is a surface roughness parameter from Choudhury et al. (1979), and τ_{veg} is vegetation optical depth.

With observations of ε_{obs} (derived from the observed T_B) and soil moisture, the value of optimal α can be determined using a linear regression with a zero intercept. Figure 3 shows a plot of the $1 - \varepsilon_{obs}$ versus $1 - \varepsilon_{soil}$ for the three areas. The values of α for H polarization are summarized in Table 2. This model approximation seems to provide an adequate explanation of the H-polarization data. However, based upon the plots of the V-polarization data shown in Fig. 3 it is apparent that the assumption of a zero intercept does not apply.

It is likely that scattering must be included in modeling the V polarization (Pampaloni and Paloscia 1986). For the V polarization we used the value of α from the H optimization and solved for ω through optimization. The form of Eq. (1) used is as follows:

$$\varepsilon_{obs} = \varepsilon_{soil}\alpha^{0.5} + (1 - \omega_{veg})(1 - \alpha^{0.5})[1 + (1 - \varepsilon_{soil})\alpha^{0.5}]. \quad (8)$$

Equation (8) is equivalent to that described in Jackson and Schmugge (1991). As explained above, the vegetation and roughness parameters have been combined into a single parameter to reduce dimensionality and to facilitate optimization. Applying this approach to all of the data from the three study areas resulted in the ω_{veg} values listed in Table 2. The values tend to increase with nominal vegetation levels and are on the order of the sparse results reported in the literature.

The performance of the soil moisture retrieval algorithm using these optimized values was determined

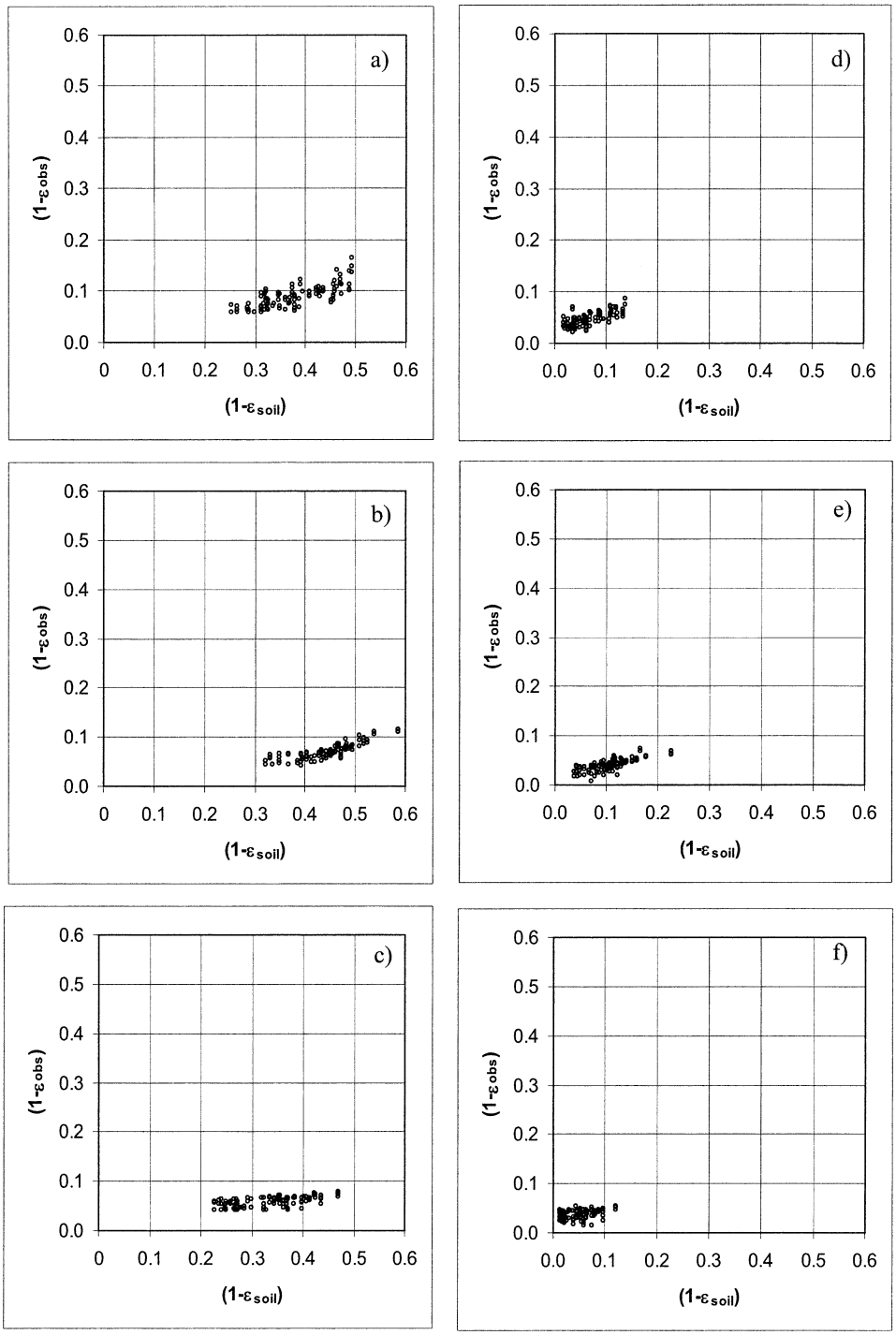

FIG. 3. Observed reflectivity and modeled soil reflectivity for 19-GHz (a) CF H, (b) ER H, (c) LW H, (d) CF V, (e) ER V, and (f) LW V.

by applying it to the observed emissivity. Standard errors of estimate are shown in Table 2. The error levels are similar to those observed by Jackson (1997). It is interesting to note that the SEE levels for CF and ER at H polarization are much higher than those resulting from a simple linear regression of emissivity and soil moisture. A possible explanation for this is the quality of the data used. The smaller sampling areas may not be representative of the footprint. Another reason may be the structure of the model itself. Prediction accuracy may be limited by the assumptions we have made.

c. Dual-polarization algorithm results

The analyses described above yielded some insight into parameter estimation and expected accuracy of the retrieval algorithm. In particular, based upon these results we estimated the values of the single-scattering albedo as 0 for H and 0.05 for V polarization. Our goal in developing the algorithm is to make it as robust as possible and minimize the necessity of any calibration. Roughness parameters were set as described previously.

The two-channel soil moisture retrieval algorithm solution we used requires the acceptance of all the assumptions listed in section 3d, the specification of the single-scattering albedo values a priori, and ancillary temperature data. Algorithm outputs are the soil moisture and the vegetation optical depth. In our implementation we also specified that the vegetation optical depth could be estimated as described in Jackson and Schmugge (1991) as a function of angle, vegetation water content, and the b parameter. Estimates of the vegetation water content were provided using ancillary data for each footprint. As a result of the process described, the algorithm provides soil moisture and an estimate of b for each footprint.

The SEE and bias for CF, ER, and LW obtained using the two-channel algorithm are listed in Table 2. SEE values for CF and LW are roughly comparable to those obtained using the linear regression approach. This gives us a degree of confidence in using the dual-polarization algorithm under the general conditions of the two areas. However, the error levels for ER are much larger than those obtained using linear regression. A substantial portion of the error is the result of the large bias. Algorithm problems associated with ER are in part related to the physical characteristics of the vegetation (which consists of thicker grassland with a layer of thatch over the surface that was less frequently grazed) and to the inadequate ground sampling size as noted in Jackson et al. (2002).

The results of the α optimization analysis and previous research results (Jackson and Schmugge 1991) can be used to evaluate the algorithm estimates of the vegetation parameter b. Average values of the vegetation parameter b derived from the algorithm were 1.16 (CF), 1.15 (ER), and 0.95 (LW). These can be compared to values presented in Jackson and Schmugge (1991). Based upon the published values these are all reasonable; however, the reliability of the CF value is questionable since vegetation effects are the lowest for this site. There was no apparent correlation between the b value and the optimized soil moisture.

It is also possible to compute a value of b from the optimized values of α listed in Table 2. In order to do this we used Eq. (6) [$h = 0.14$ as presented in Njoku and Li (1999)] and mean values of the vegetation water content for each site. In addition, an angular correction was performed (Jackson and Schmugge 1991). The values obtained for b were 1.06 (CF), 0.86 (ER), and 1.14 (LW). These values are on the order of those reported in the literature at 19 GHz (Pampaloni and Paloscia 1986).

To illustrate the applicability of the algorithm to mapping and the potential information content of the resulting products, we generated map images for each SSM/I overpass. For each overpass, soil moisture was estimated for every footprint. These data were input to a mapping routine that used a kriging-based interpolation to generate an 800-m gridded product. Figure 4 is a subset of the over 100 datasets available. This set, collected during 1999, was selected to illustrate a dry-down sequence during which a large rainfall event occurred on 9–10 July (see Fig. 1). The urban area around Oklahoma City was extracted from the data before retrieval.

7. Conclusions

Previous studies have suggested that microwave data with frequencies higher than 10 GHz are not appropriate for soil moisture estimation since the vegetation will strongly mask surface information. However, a number of investigations using SSM/I data have presented evidence that there is a usable soil moisture signal under some conditions. Much of this work has been qualitative in nature, relying on indices and not the surface soil moisture for validation.

There are well-established theories describing the microwave emission of the land surface. Vegetation is important in these models but is less significant at low frequencies. At higher frequencies the vegetation is a more dominant feature, and soil moisture retrievals are more sensitive to the representation and parameterization of vegetation effects. Estimating algorithm parameters a priori, as suggested for low frequencies, may not be reliable. For this reason we evaluated a retrieval technique utilizing dual-polarization observations.

Data collected in two field experiments in the Southern Great Plains of the United States were used with SSM/I measurements to better understand the behavior of soil moisture and emissivity at these higher frequencies. The region used for the investigation was well suited to the limitations of using 19-GHz data to estimate soil moisture.

For each of three study areas, a linear relationship was observed between soil moisture and emissivity. Areas with lighter vegetation and the use of H-polarization data produced better linear regression results based on correlation and standard error of estimate values.

An attempt was made to describe the observed linear trends using a radiative transfer model in which the vegetation parameters were optimized. This is essentially the same as using the single-polarization approach described in Jackson (1997). Analysis resulted in values of the vegetation optical depth and the single-scattering albedo that were reasonable based upon published data. The single-channel algorithms had higher SEE than the linear regressions but low bias. These results suggest that there is a limitation on accuracy that is attributed

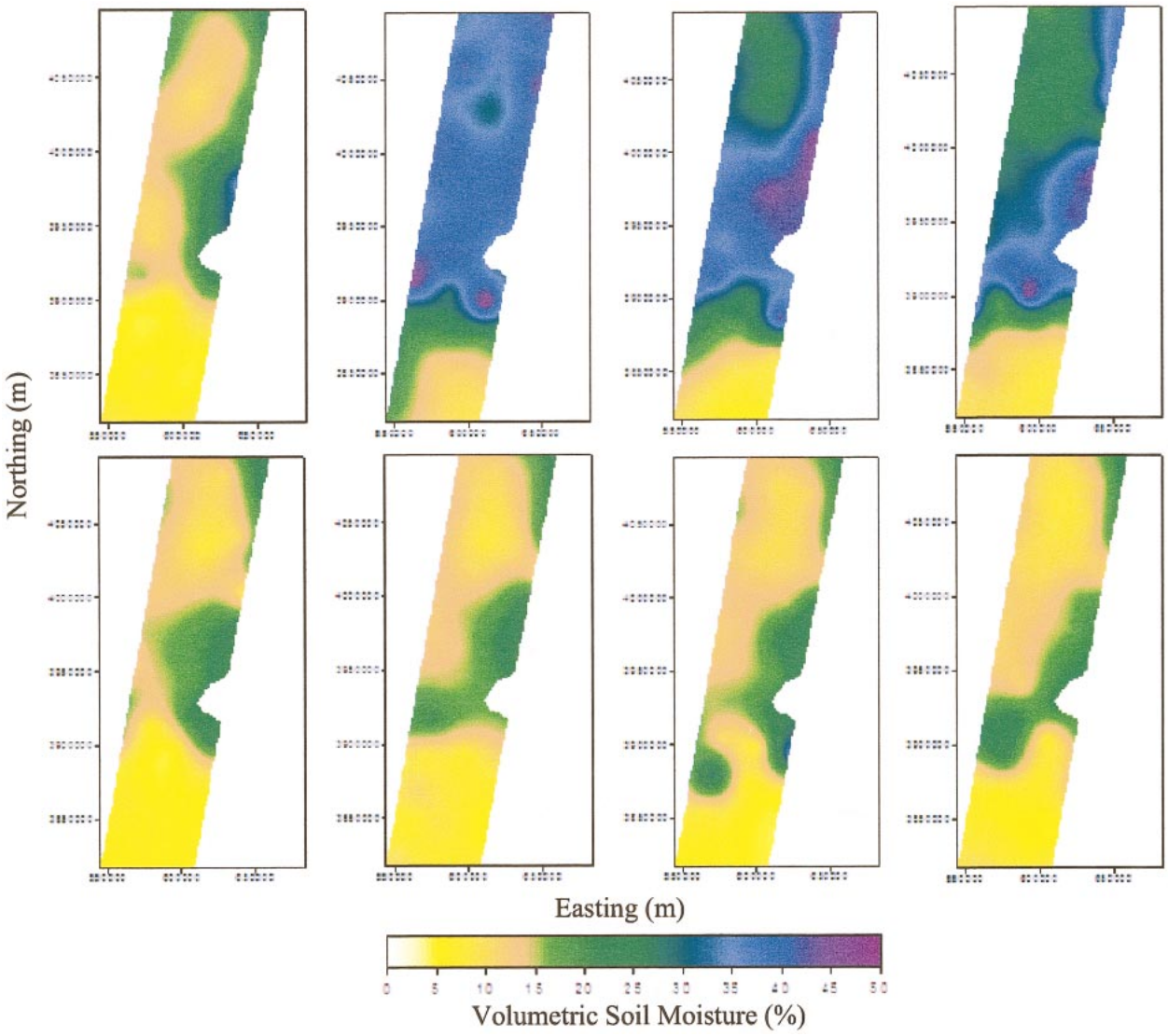

FIG. 4. Soil moisture images based upon dual-polarization algorithm retrievals.

to either the model structure or the quality of the ground observations. Both causes are considered possible.

The dual-polarization algorithm explicitly incorporates parameters that were lumped in the single-channel optimization. It utilizes the same equations but makes assumptions about the effects of polarization on some parameters. If these assumptions on vegetation effects are valid, it is a potentially robust solution. The most significant problem in applying this approach is reducing the number of unknowns to two (i.e., soil moisture and the vegetation parameter *b*).

The availability of data to perform atmospheric corrections and to estimate effective soil temperature at the time of SSM/I observation may add some restrictions to the application of this approach to areas without meteorological network and radiosonde observations. As an alternative to estimating temperature, van de Griend (2001) demonstrated that effective temperature could be estimated using 37-GHz V-polarization brightness temperature and some climatologic records over semiarid areas. The *Aqua* satellite, recently launched by NASA, includes sensors that can provide atmospheric profile information. With these additional measurements this approach can be extended to other areas with sparse vegetation.

An error analysis of the dual-polarization algorithm revealed that it produced good results for two of the test areas (CF and LW) but poor results at ER. This is attributed to the sources of error identified in previous investigations (Jackson et al. 2002).

Subject to the assumptions made in its implementation, the dual-polarization algorithm worked well in these tests with SSM/I data. We acknowledge that conditions in the SGP region are benign for the frequency

used. However, it is anticipated that with lower-frequency channels available with AMSR that the assumptions and limitations imposed by vegetation on soil moisture estimation will be improved.

Acknowledgments. The authors would like to thank those individuals who participated in the Southern Great Plains 1997 and 1999 hydrology experiments. This investigation was possible because of exceptional efforts of the soil moisture sampling teams that went out every day. We also acknowledge the ARM Program sponsored by the U.S. Department of Energy for providing radiosonde data, the NASA/NOAA Pathfinder Programs for providing NDVI data derived from AVHRR, and NOAA NESDIS for providing the SSM/I data. Portions of this work were supported by the NASA Land Surface Hydrology Program and the NASDA *ADEOS-II* project.

REFERENCES

Ahmed, N. U., 1995: Estimating soil moisture from 6.6 GHz dual polarization, and/or satellite derived vegetation index. *Int. J. Remote Sens.,* **16,** 687–708.

Calvet, J.-C., J.-P. Wigneron, A. Chanzy, and D. Haboudane, 1995: Retrieval of surface parameters from microwave radiometry over open canopies at high frequencies. *Remote Sens. Environ.,* **53,** 46–60.

Choudhury, B. J., and R. E. Golus, 1988: Estimating soil wetness using satellite data. *Int. J. Remote Sens.,* **9,** 1251–1257.

——, T. J. Schmugge, A. Chang, and R. W. Newton, 1979: Effect of surface roughness on the microwave emission from soils. *J. Geophys. Res.,* **84,** 5699–5706.

——, ——, and T. Mo, 1982: A parameterization of effective temperature for microwave emission. *J. Geophys. Res.,* **87,** 1301–1304.

Dobson, M. C., F. T. Ulaby, M. T. Hallikainen, and M. A. El-Rayes, 1985: Microwave dielectric behavior of wet soil. II. Dielectric mixing models. *IEEE Trans. Geosci. Remote Sens.,* **23,** 35–46.

Drusch, M., E. F. Wood, and T. J. Jackson, 2001: Vegetative and atmospheric corrections for the soil moisture retrieval from passive microwave remote sensing data: Results from the Southern Great Plains Hydrology Experiment 1997. *J. Hydrometer.,* **2,** 181–192.

Hallikainen, M. T., F. T. Ulaby, M. C. Dobson, M. A. El-Rayes, and L. K. Wu, 1985: Microwave dielectric behavior of wet soil. Part I: Empirical models and experimental observations. *IEEE Trans. Geosci. Remote Sens.,* **23,** 25–34.

Hollinger, J. P., J. L. Peirce, and G. A. Poe, 1990: SSM/I instrument evaluation. *IEEE Trans. Geosci. Remote Sens.,* **28,** 781–790.

Jackson, T. J., 1993: Measuring surface soil moisture using passive microwave remote sensing. *Hydrol. Processes,* **7,** 139–152.

——, 1997: Soil moisture estimation using special satellite microwave/imager satellite data over a grassland region. *Water Resour. Res.,* **33,** 1475–1484.

——, and T. J. Schmugge, 1991: Vegetation effects on the microwave emission of soil. *Remote Sens. Environ.,* **36,** 203–212.

——, and A. Y. Hsu, 2001: Soil moisture and TRMM microwave imager relationships in the Southern Great Plains 1999 (SGP99) experiment. *IEEE Trans. Geosci. Remote Sens.,* **39,** 1632–1642.

——, D. M. Le Vine, A. Y. Hsu, A. Oldak, P. J. Starks, C. T. Swift, J. D. Isham, and M. Haken, 1999: Soil moisture mapping at regional scales using microwave radiometry: The Southern Great Plains Hydrology Experiment. *IEEE Trans. Geosci. Remote Sens.,* **37,** 2136–2151.

——, A. Oldak, A. Gaswieski, M. Klein, E. G. Njoku, A. Yevgrafov, S. Christiani, and R. Bindlish, 2002: Soil moisture retrieval using the polarimetric scanning radiometer C band in the Southern Great Plains 1999 experiment. *IEEE Trans. Geosci. Remote Sens.,* in press.

Kirdiashev, K. P., A. A. Chukhlantsev, and A. M. Shutko, 1979: Microwave radiation of the Earth's surface in the presence of vegetation cover. *Radio Eng. Electron. Phys.* (English translation), **24,** 256–264.

Koike, T., E. Njoku, T. J. Jackson, and S. Paloscia, 2000: Soil moisture algorithm development and validation for the ADEOS-II/AMSR. *Proc. 2000 Int. Geoscience and Remote Sensing Symp.,* Honolulu, HI, IEEE Geoscience and Remote Sensing Society, IEEE Catalog 00CH37120, 1253–1255.

Lakshmi, V., E. F. Wood, and B. J. Choudhury, 1997: Evaluation of SSM/I satellite data for regional soil moisture estimation over the Red River basin. *J. Appl. Meteor.,* **36,** 1309–1328.

Liebe, H. J., G. A. Hufford, and M. G. Cotton, 1993: Propagation modeling of moist air and suspended water/ice particles at frequencies below 1000 GHz. *Proc. AGARD 52d Specialists Meeting of Electromagnetic Wave Propagation Panel,* Palma de Mallorca, Spain, AGARD, 3.1–3.10.

Morland, J. C., D. I. Grimes, and T. J. Hewison, 2001: Satellite observations of the microwave emissivity of a semi-arid land surface. *Remote Sens. Environ.,* **22,** 149–164.

Njoku, E. G., and L. Li, 1999: Retrieval of land surface parameters using passive microwave measurements at 6 to 18 GHz. *IEEE Trans. Geosci. Remote Sens.,* **37,** 79–93.

——, T. Koike, T. J. Jackson, and S. Paloscia, 2000: Retrieval of soil moisture from AMSR data. *Microwave Radiometry and Remote Sensing of the Earth's Surface and Atmosphere,* P. Pampaloni and S. Paloscia, Eds., VSP Publications, 525–533.

Owe, M., A. A. van de Griend, and A. T. C. Chang, 1992: Surface moisture and satellite microwave observations in semiarid southern Africa. *Water Resour. Res.,* **28,** 829–839.

Paloscia, S., and P. Pampaloni, 1992: Microwave vegetation indexes for detecting biomass and water conditions of agricultural crops. *Remote Sens. Environ.,* **40,** 15–26.

——, ——, L. Chiarantini, P. Coppo, S. Gagliani, and G. Luzi, 1993: Multifrequency passive microwave remote sensing of soil moisture and roughness. *Int. J. Remote Sens.,* **14,** 467–483.

Pampaloni, P., and S. Paloscia, 1986: Microwave emission and plant water content: A comparison between field measurements and theory. *IEEE Trans. Geosci. Remote Sens.,* **24,** 900–905.

Schmugge, T. J., T. J. Jackson, W. P. Kustas, and J. R. Wang, 1992: Passive microwave remote sensing of soil moisture: Results from HAPEX, FIFE and MONSOON 90. *ISPRS J. Photogramm. Remote Sens.,* **47,** 127–143.

Teng, W. L., J. R. Wang, and P. C. Doraiswamy, 1993: Relationship between satellite microwave radiometric data, antecedent precipitation index, and regional soil moisture. *Int. J. Remote Sens.,* **14,** 2483–2500.

Ulaby, F. T., M. Razani, and M. C. Dobson, 1983: Effects of vegetation cover on the microwave radiometric sensitivity of soil moisture. *IEEE Trans. Geosci. Remote Sens.,* **21,** 51–61.

van de Griend, A. A., 2001: The effective thermodynamic temperature of the emitting surface at 6.6 GHz and consequences for soil moisture monitoring from space. *IEEE Trans. Geosci. Remote Sens.,* **39,** 1673–1679.

Vinnikov, K. Y., A. Robock, S. Qiu, J. K. Entin, M. Owe, B. J. Choudhury, S. E. Hollinger, and E. G. Njoku, 1999: Satellite remote sensing of soil moisture in Illinois, USA. *J. Geophys. Res.,* **104,** 4145–4168.

Wang, J. R., 1985: Effect of vegetation on soil moisture sensing observed from orbiting microwave radiometers. *Remote Sens. Environ.,* **17,** 141–151.

——, and T. J. Schmugge, 1980: An empirical model for the complex dielectric permittivity of soils as a function of water content. *IEEE Trans. Geosci. Remote Sens.,* **18,** 288–295.